SANDIA REPORT

SAND2015-8444
Unlimited Release
Printed September 2015

Electrically Injected UV-Visible Nanowire Lasers

George T. Wang, Changyi Li, Qiming Li, Sheng Liu, Jeremy B. Wright, Igal Brener, Ting-Shan Luk, Weng W. Chow, Benjamin Leung, Jeffrey J. Figiel, Daniel D. Koleske, Tzu-Ming Lu

Prepared by
Sandia National Laboratories
Albuquerque, New Mexico 87185 and Livermore, California 94550

Sandia National Laboratories is a multi-program laboratory managed and operated by Sandia Corporation, a wholly owned subsidiary of Lockheed Martin Corporation, for the U.S. Department of Energy's National Nuclear Security Administration under contract DE-AC04-94AL85000.

Issued by Sandia National Laboratories, operated for the United States Department of Energy by Sandia Corporation.

Available to DOE and DOE contractors from
U.S. Department of Energy
Office of Scientific and Technical Information
P.O. Box 62
Oak Ridge, TN 37831

Telephone: (865) 576-8401
Facsimile: (865) 576-5728
E-Mail: reports@osti.gov
Online ordering: http://www.osti.gov/scitech

Available to the public from
U.S. Department of Commerce
National Technical Information Service
5301 Shawnee Rd
Alexandria, VA 22312

Telephone: (800) 553-6847
Facsimile: (703) 605-6900
E-Mail: orders@ntis.gov
Online order: http://www.ntis.gov/search

SAND2015-8444
Unlimited Release
Printed September 2015

Electrically Injected UV-Visible Nanowire Lasers

George T. Wang*, Changyi Li, Qiming Li, Sheng Liu, Jeremy B. Wright, Igal Brener, Ting-Shan Luk, Weng W. Chow, Benjamin Leung, Jeffrey J. Figiel, Daniel D. Koleske, Tzu-Ming Lu, Donald Bethke
*E-mail: gtwang@sandia.gov

Sandia National Laboratories
P.O. Box 5800
Albuquerque, New Mexico 87185-MS1086

Abstract

There is strong interest in minimizing the volume of lasers to enable ultracompact, low-power, coherent light sources. Nanowires represent an ideal candidate for such nanolasers as stand-alone optical cavities and gain media, and optically pumped nanowire lasing has been demonstrated in several semiconductor systems. Electrically injected nanowire lasers are needed to realize actual working devices but have been elusive due to limitations of current methods to address the requirement for nanowire device heterostructures with high material quality, controlled doping and geometry, low optical loss, and efficient carrier injection. In this project we proposed to demonstrate electrically injected single nanowire lasers emitting in the important UV to visible wavelengths. Our approach to simultaneously address these challenges is based on high quality III-nitride nanowire device heterostructures with precisely controlled geometries and strong gain and mode confinement to minimize lasing thresholds, enabled by a unique top-down nanowire fabrication technique.

ACKNOWLEDGMENTS

We thank Mary H. Crawford, Daniel Feezell, Steven R. J. Brueck, and Antonio Hurtado for helpful technical discussions and suggestions. This work was performed, in part, at the Center for Integrated Nanotechnologies, an Office of Science User Facility operated for the U.S. DOE, Office of Science. This work was supported by the Laboratory Directed Research and Development program at Sandia National Laboratories.

CONTENTS

FIGURES

NOMENCLATURE

DOE	Department of Energy
SNL	Sandia National Laboratories
NW	Nanowire
GaN	Gallium Nitride
InGaN	Indium Gallium Nitride
MQW	Multiple Quantum Well
DBR	Distributed Bragg Reflector
STEM	Scanning Transmission Electron Microscopy
SEM	Scanning Electron Microscopy
μ-PL	Micro-photoluminescence
MOCVD	Metal-Organic Chemical Vapor Deposition
I-V	Current-Voltage
RTA	Rapid Thermal Anneal

1. INTRODUCTION

Semiconductor nanowires (NWs) are attractive candidates for ultracompact and low-power nanoscale lasers, being able to simultaneously function as a standalone optical cavity and gain medium. Nano-enabled advantages of NW lasers include an extremely high mode confinement due to a high index and nanoscale diameter and strain relaxation enabling lower extended defect density and a wider alloy/bandgap space. Unique architectures such as radial quantum wells are also possible in NW geometries. NW lasing via optical pumping has been demonstrated in several material systems, but electrically injected lasing needed for actual devices has proven much more difficult. Lasing from an electrically injected CdS NW was reported in 2003*[1]*, but the relative lack of successful follow-on reports for single NW lasers almost a decade later, despite high interest, later underscores the non-trivial nature in realizing electrically injected NWs lasers, including in the technologically important III-nitride materials system which commercial blue/green LEDs and laser diodes are based on.

In contrast to optically-pumped lasing where the excitation efficiency can approach unity, lasing via electrical injection is considerably more challenging as electrons and holes need to be injected separately and efficiently transported to and recombined in the active region. Technical challenges that make electrically injected lasing in a NW geometry particularly difficult include relatively low end facet reflectivities and the need for low defect densities, n- and p-type doped heterojunctions, control of the NW dimensions, and good electrical contacts and efficient electrical transport. Current, state-of-the art "bottom-up" NW growth techniques are poorly suited for overcoming these challenges due to limitations caused by necessarily narrow range of anisotropic growth conditions, which leads to issues in limiting point defect densities, creating arbitrary heterostructures (e.g. can create either axial or radial architectures, but not both), size uniformity, and doping (potentially incompatible growth conditions). Current top-down methods using a plasma etch are also ill-suited as they result in tapered geometries with high defect densities from etch damage.

In this project, we took an integrated experimental and theoretical approach to simultaneously address the materials, optical, and device issues that need to be overcome to achieve electrically injected lasers based on III-nitride NWs, which have the desirable properties of high crystalline quality, low surface recombination velocity, high breakdown current, and tunable direct bandgaps in the UV to visible wavelengths. Our distinguishing and enabling approach is based on a novel top-down NW fabrication technique we have recently developed (unique to Sandia) that significantly improves on current state-of-the art methods. Novel strategies to reduce lasing thresholds including the use of NW distributed Bragg reflector (DBR) structures and metal end facet mirrors to enhance the cavity reflectivity were explored. Theory and modeling were closely integrated with the experiments to help design NW heterostructures with minimal lasing thresholds and to understand and predict the properties and physics from these nanolasers. The effects of size and placement of metal contacts on the NW lasing properties and carrier transport were also explored.

2. PROJECT GOALS

Our overall goal was to demonstrate an electrically injected, monolithic single nanowire laser. By having the p-i-n regions entirely incorporated as part of the nanowire laser heterostructure itself, integration into arbitrary platforms becomes possible. In order to overcome the numerous challenges to reach this goal, work was organized under three primary Tasks as follows.

Task 1: Nanowire Laser Fabrication
Goal: Design and fabricate optimal p-i-n junction InGaN/GaN MQW (multi-quantum well) nanowire laser structures for electrical injection

- Success measures: realize optimal NW design(s) with necessary control of: size, heterostructure architecture, n- and p-doping, and emission wavelength (bandgap).

Task 2: Threshold Reduction and Optical Characterization
Goal: Reduce nanowire lasing thresholds via enhancement of end facet reflectivities and optimal active region placement

- Success measures: demonstration of optically pumped lasing and continual reduction of lasing thresholds, as measured by optical pumping experiments.

Task 3: Device Fabrication and Electrical Injection
Goal: Demonstrate electrically injected nanowire laser in the UV or visible wavelengths

- Success measures: understanding effect of contacts on optical properties; demonstration of Ohmic contacts and electrically injected luminescence (subthreshold) will provide evidence of progress toward success.

3. KEY ACCOMPLISHMENTS

3.1 Nanowire Laser Fabrication

The basis for our nanowire fabrication is a top-down process, in contrast to typically bottom-up grown nanowires. The unprecedented flexibility of this new capability, which combines an inductively coupled plasma (ICP) dry etch with an selective KOH-based wet etch, allows us to create and evaluate high quality NW laser heterostructures with controlled geometries and architectures, including both axial and radial type multi-quantum well (MQW) active regions, n- and p-type doping, and tunable bandgaps. We have demonstrated optically pumped single-mode lasing in n-type GaN nanowires created by this method with thresholds less than 200 kW/cm^2 (Fig. 1a). Here we employed GaN/InGaN multi-quantum wells (MQWs) as the active region to maximize carrier capture and recombination, as done in GaN-based LEDs and laser diodes. Both axial*[2]* and radial-type*[3]* p-n junction MQW NW heterostructure architectures, which we have demonstrated using our top-down method (Fig. 1b and 1c), were explored for greatest design flexibility, as each architecture has pros and cons that will be investigated. For example, NW and electrical device fabrication is simpler for axial geometries, but radial designs provide larger active region volumes and potentially higher injection efficiencies*[4]*.

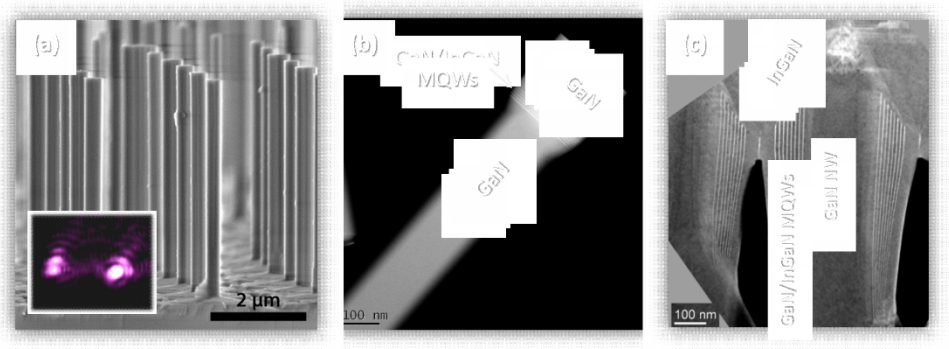

Figure 1. (a) n-GaN NWs fabricated by top-down method and CCD lasing image from NW ends (inset); (b) axial and (c) radial type MQW p-n junction NWs (STEM images)

3.1.1 Axial Nanowire Fabrication

During this project, we significantly improved our control over the NW diameter fabricated with our top-down process by using electron-beam (e-beam) lithography instead of silica sphere lithography to define the etch masks. For p-i-n axial NW architectures, the different wet etch rates of the p- and n-type GaN results in considerable tapering, as seen in Fig. 1(b). This tapering is undesired for nanowire lasers due to increased optical losses and increased difficulties in making electrical contacts. By using e-beam lithography to define Ni dots as etch masks close to the targeted diameters, minimal wet etching to remove etch damage and straighten and smooth the sidewalls was required, limiting the resulting taper. Fig. 2 shows axial nanowire p-i-n InGaN/GaN MQW nanowires fabricated using this approach.

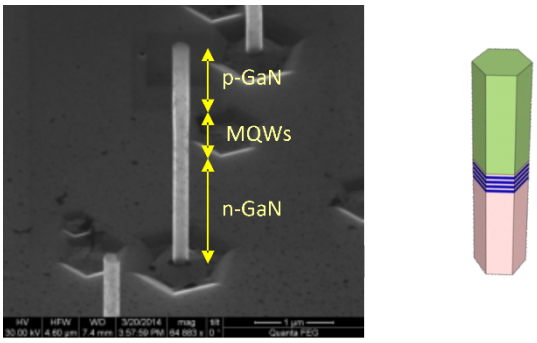

Figure 2. Axial nanowire design fabricated by improved top-down approach

3.1.2 Radial Nanowire Fabrication

Radial, or core-shell, InGaN/GaN MQW p-i-n nanowires were also realized through a combination of top-down fabrication to create n-type GaN nanowire cores (diameter ~150-250 nm) from n-type GaN epilayers grown on c-plane sapphire, followed by regrowth in a metal-organic chemical vapor deposition (MOCVD) reactor to create the active region (InGaN/GaN MQWs), AlGaN electron blocking layer, and finally p-GaN shell layer. Several regrowth recipes were performed, with changes to the MQW thicknesses, growth temperature, and other parameters. Figure 3 shows a representative scanning electron microscopy (SEM) image of a radial p-i-n nanowire following regrowth. We note the slight taper, with decreasing diameter from tip to base, likely caused by a faster growth rate at the nanowire tip. This will likely increase optical loss in the nanowire cavity, and future work should be aimed at minimizing this taper.

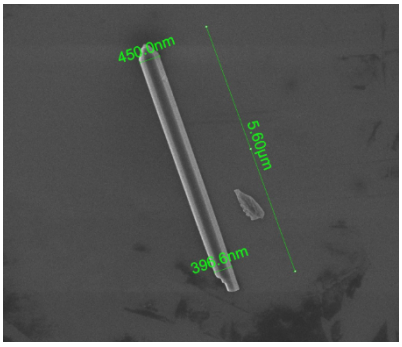

Figure 3. SEM image of radial p-i-n InGaN/GaN nanowire

3.2 Threshold Reduction and Optical Characterization

In this task strategies and designs for reducing the threshold gain of the NW lasers were explored. The threshold gain g_{th} can be written as $g_{th}=\alpha/\Gamma$, where Γ is the mode confinement factor, and α represents the total optical losses. To reduce g_{th} to achieve lower current injection requirements for lasing, one must minimize α and maximize Γ. The primary optical loss mechanism comes from the end facet emission of the NW, with $\alpha\cong(1/L)\ln(1/R_1R_2)$. We proposed

to improve the cavity feedback by exploring the novel use of distributed Bragg reflectors (DBRs) in the context of NWs. We have identified two potential paths to achieve a DBR NW laser: The first is to use built-in DBR mirrors at the NW ends via axial heterostructuring multiple periods of alternating GaN/AlN layers via our top-down fabrication method. Planar DBRs based on a GaN/AlN stack have shown peak reflectance of up to 95% at 392 nm *[5]* and are being used in III-nitride VCSELs. The second approach is to couple the NW to nano-patterned DBR gratings external to the cavity. These two approaches are shown schematically in Figure 4. The intra-cavity (built-in) approach is preferred for greater device integration flexibility and compactness. A second approach to reduce g_{th} is to maximize Γ, using geometrical tuning to realize optical modes that maximize the spatial overlap with the gain region. We also explored the use of deposited Al end mirrors to enhance the end facet reflectivities. Commercial fully vectorial eigenvalue mode solver simulations (Lumerical) were used to model the modes of the NW waveguide to guide NW laser designs with high Γ. These models help to determine the optimal placing of InGaN QWs within the NW. The optical properties of the NWs were characterized using a micro-photoluminescence (μ-PL) setup. Details of the optical characterization setup can be found elsewhere.*[6, 7]*

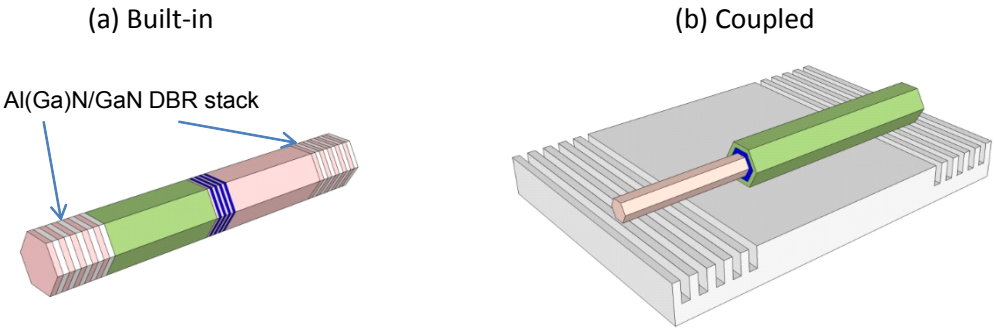

Figure 4. Schemes for (a) built-in DBR stack within the nanowire laser and (b) nanowire laser coupled to an external grating.

3.2.1 Built-in DBR Nanowire Laser

We explored the possibility of fabricating nanowire lasers with built-in DBRs at the ends of the nanowire, as drawn in Fig. 4, which, being monolithic, is advantageous for integration purposes. Planar GaN/AlN DBR designs were modeled via a custom Matlab code and then grown by metal-organic chemical vapor deposition, leading to heterostructure films with >75% reflectivity at 433 nm from a single DBR stack, which is close to our targeted design. We also successfully grew a planar heterostructure incorporating two DBR stacks and an InGaN/GaN multi-quantum well active region, a nontrivial accomplishment given the high inherent strain in these heterostructures. Using our top-approach, we attempted to etch axial NW lasers with the built-in DBRs at both end facets from this planar heterostructure. However, significant difficulties were encountered with this approach. Using a hexagonal, close-packed silica sphere etch mask, a stepped wire morphology, with skinnier top and fatter bottom, was observed following the ICP etch and wet etch, as shown in Fig. 5(b). Moving to 500 nm diameter Ni dots as an etch mask, patterned by interferometric lithography, resulted in a less stepped NW morphology, as shown in Fig. 5(c); however, the morphology is still not adequately straight to be suitable for lasing. Although the cause of the stepped structure is still under investigation, it may be caused by the InGaN/GaN MQW stack interfering the with the etch process.

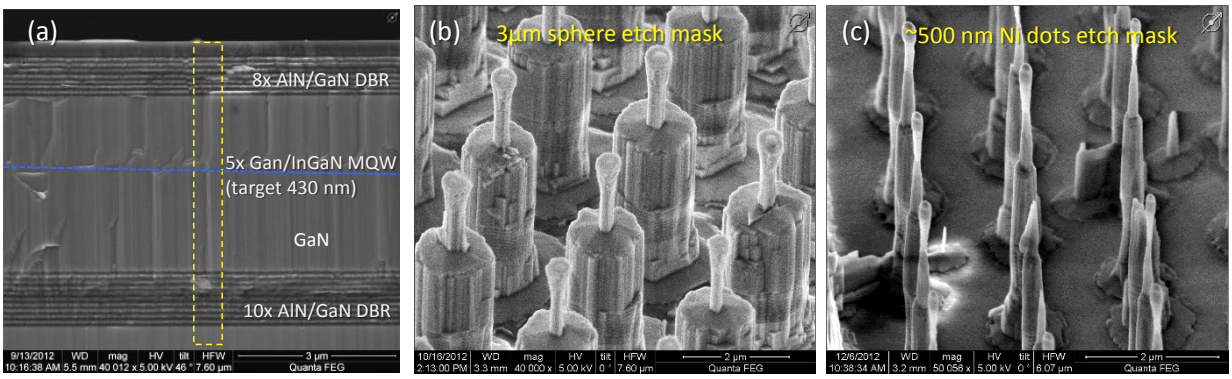

Figure 5. (a) Planar dual AlN/GaN DBR heterostructure with InGaN/GaN MQW active region. (b), (c) Stepped wires fabricated from planar heterostructure in (a) using silica spheres or Ni dots as etch masks.

3.2.2 Coupled Distributed Feedback Nanowire Laser

We also explored coupling a GaN NW to an external dielectric grating to achieve distributed feedback, which is a proven technique for mode selection in semiconductor lasers. The effective periodicity of the grating experienced by the NW was altered using nanomanipulation to change the angular alignment between the NW and the grating. The effective periodicity controls the spectral location of the distributed feedback stop-band. Single mode emission was achieved at an alignment, where the designed periodicity of the grating was experienced by the NW. Using an in-situ SEM nanomanipulator, we studied the lasing properties of the NW as a function of rotation angle with respect to the grating. Whereas the NW exhibits multi-mode lasing when aligned with the grating, rotating the NW perpendicular to the grating leads to single-mode lasing, which is advantageous for device characteristics. Only a slight reduction in the lasing threshold was observed, however, potentially due to losses from interaction with the grating. Further details are published elsewhere.*[8]*

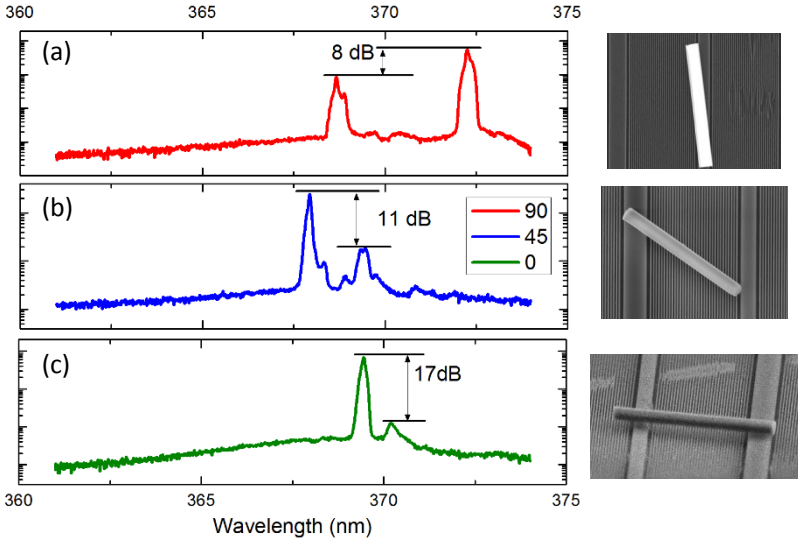

Figure 6. Lasing spectra measured with a single GaN nanowire aligned (a) parallel, (b) angled, or (c) perpendicular to an underlying dielectric grating. Single mode lasing emission is obtained when the nanowire is perpendicular to the grating, as shown in (c).

3.2.3 *Aluminum End Facet Mirrors on Nanowire Lasers*

Due to the difficulty in growing and fabricating NW lasers with built-in DBRs, we subsequently explored the use of Al to enhance the end facet reflectivities. Finite difference time domain (FDTD) simulations (Lumerical) performed for a GaN NW with a 300 nm diameter and emission wavelength of 400 nm show a significant enhancement of the reflectivity up to ~90% for the TE_{01} mode by adding a 50 nm Al mirror to the end facet, compared to ~70% for the bare NW facet. E-beam deposition of Al was performed at either one or both ends for several individual GaN NWs lying on sapphire substrates, as shown in Fig. 7. Optical characterization of bare NWs and NWs with either one or both ends coated with Al were performed, as shown in Fig. 7(c). The results show no significant difference in average lasing threshold by optical pumping with Al at the end facets. The lack of threshold reduction may result from propagation losses caused by Al being deposited on the NW sidewalls at the NW ends. Thus, future work should try to limit Al deposition to solely the end facets.

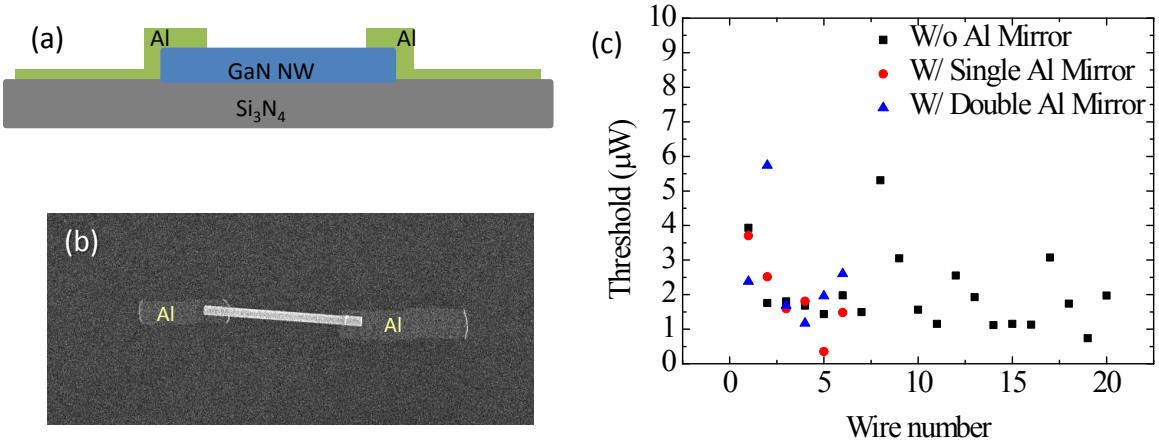

Figure 7. (a) Side-view schematic of Al end mirrors on GaN NW laser. (b) top-view SEM image of Al deposited on end-facets. (c) lasing thresholds of bare GaN NWs and GaN NWs with either one or both Al end mirrors, showing no significant differences.

3.2.4 *Optical characterization of axial and radial InGaN/GaN MQW p-i-n nanowires*

Single p-i-n axial InGaN/GaN MQW NWs fabricated as described in 3.1.1 were optically characterized using μ-PL. As seen in Fig. 8, lasing from only the GaN portion of the NW is observed, rather than from the InGaN/GaN MQW active region. The small volume of the InGaN disks comprising the active region is likely insufficient to provide enough gain to achieve lasing even under optical pumping. We conclude that lasing from this axial architecture would most likely require unrealistic end facet reflectivities close to one.

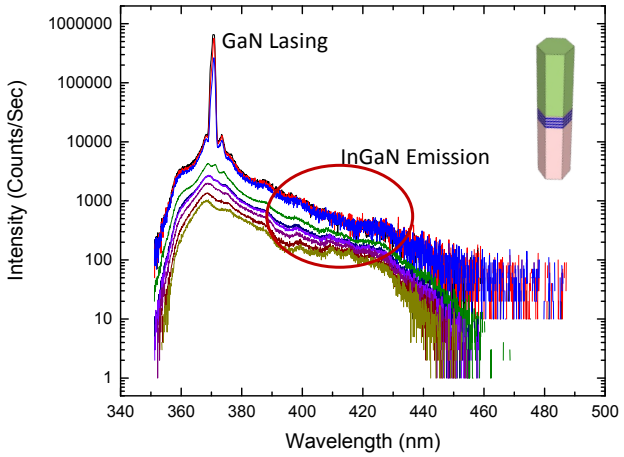

Figure 8. Optical emission spectra from an axial p-i-n InGaN/GaN MQW NW

Based on this finding, we moved our focus to the radial NW architecture, which provides a much larger gain region due to the large volume of the InGaN shells versus InGaN disks in the axial architecture. Radial p-i-n InGaN/GaN MQW NWs were fabricated as described in 3.1.2. Under optical pumping, we were able to observe lasing from single radial NWs, as shown in Fig. 9. This result confirms that sufficient gain in present in the radial architecture to achieve lasing, in contrast to the axial architecture. Further details will be provided in a manuscript under preparation.

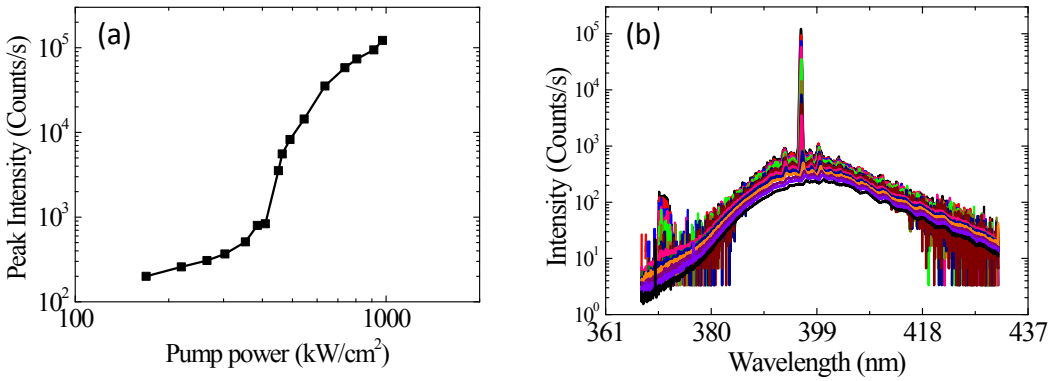

Figure 9. (a) Peak intensity measured versus optical pump power for a radial NW. (b) Optical emission spectra, showing onset of lasing.

3.3 Device Fabrication and Electrical Injection

In this task we demonstrated electrical injection into our NWs using different NW contact schemes. Specially designed NW test platforms (SiO_2/Si) with predefined contact pads fabricated by optical lithography were utilized. As-fabricated NWs were removed from their original substrate and dry transferred to the platforms using a swab. Metal contact lines from these predefined contact pads were defined by e-beam lithography for electrical injection. Much of our effort was focused on demonstrating Ohmic contacts to the n- and p- regions of the NW. Figure

10 shows Ti contacts made to the ends of a single n-type GaN NW, and corresponding current-voltage (I-V) plot, which shows Ohmic behavior. While we were able to achieve Ohmic n-type contacts to n-type GaN NWs, attempting to demonstrate p-type NW contacts proved to be much more challenging.

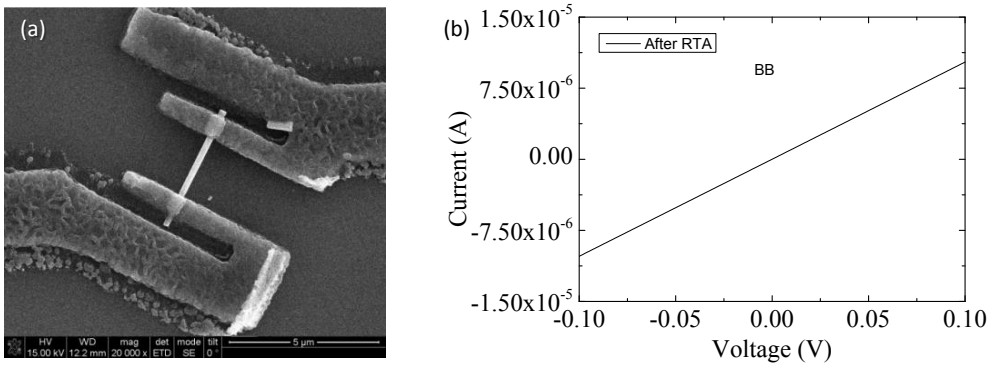

Figure 10. (a) SEM image of 400 nm thick Ti contacts patterned on a single n-type GaN NW, followed by rapid thermal anneal (RTA) at 850 °C for 30s in forming gas. (b) I-V characteristics of a n-type GaN NW device, exhibiting Ohmic behavior.

For p-type contact development, p-type GaN NWs were fabricated using our top-down approach from a ~1.5 μm p-type GaN film grown by MOCVD. A number of different contact metallization schemes and RTA recipes were tested on individual p-type GaN NWs, and electrical characterization was carried out on the resulting NW devices. Prior to metal contact deposition, the NWs were typically treated in 2% HF solution or HCl:H_2O 1:1 solution to remove any potential surface oxide. Despite successful demonstration of Ohmic contacts to the p-type GaN film the p-type NWs were etched from, similar contact metallization recipes of individual nanowires did not result in Ohmic behavior. Observed currents for single p-type GaN NW devices ranged from pA to nA range at ~1-3V. Different contact metallization schemes attempted included Ni, Ni/Au, Ti/Au/Pt, Ti/Ni/Au, Ge/Ag, and sputtered indium-tin-oxide (ITO).

Electrical contacts were subsequently fabricated on radial core-shell p-i-n InGaN/GaN MW NWs. A representative contacted NW is shown in Figure 11(a). Ti was deposited as the n-type contact to the open end (based) of the core-shell nanowire, making contact to the inner n-type core. While the Ti contact contacts the p-type shell region as well, the high resistance of the p-type GaN shell prevents shorting to the p-type contact. Due to low conductivity of the p-GaN shell layer, a current spreading layer, comprised of 5 nm Ni/ 5 nm Au, was patterned by e-beam lithography, prior to deposition of the primary Ni/Au p-contact line. Electroluminescence from the InGaN MQWs was successfully observed from this device, with increasing intensity with increasing device current. However, lasing was not observed before the device was destroyed by Joule heating at ~ 1mA continuous current. In order to reduce heating, a pulsed electrical injection scheme was implemented, with a 0.5% duty cycle (300 μs and 0.06 s period). Electroluminescence was again observed, but lasing was not observed up to currents of 2mA.

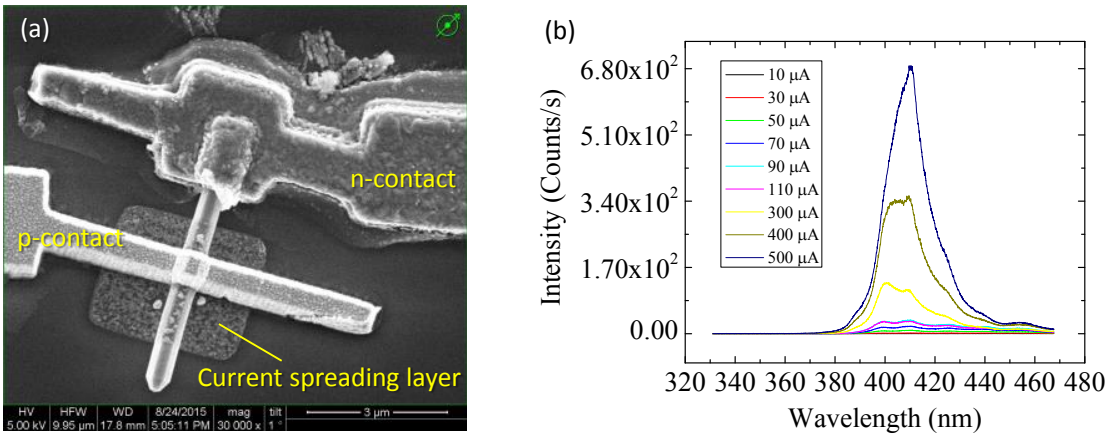

Figure 11. (a) SEM image showing contacts made to radial core-shell p-i-n NW diode. (b) Electroluminescence spectra from NW LED device shown in (a).

The presence of metal contacts on a large portion of the nanowire surface may also be expected to result in optical losses that could increase lasing thresholds. In order to better study this effect, the optically pumped lasing thresholds of several radial p-i-n nanowires were measured at various steps of the contact fabrication process. We note that the metal contacts absorb or reflect some of the incoming pump light, so the detrimental effect of the metal contacts on true lasing thresholds will be overestimated by this method. Of 8 NWs tracked, only 2 still lased after deposition of the Ti n-contact, with one NW showing an approximate tripling in lasing threshold. However, after RTA of the Ti contact, 2 NWs recovered and were able to lase via optical pumping. Interestingly, Two of the four NWs showed lower thresholds following RTA of the Ti contact than the initial bare NW. Upon subsequent deposition of a Ni/Au current spreading layer and subsequent RTA, only 2 of the original 8 NWs were able to lase, although one of the NWs had a lower threshold than before any metal contacts were deposited on it. The results indicate that the placement and type of metal contacts needs to be carefully considered to minimize optical losses, while simultaneously maximizing electrical injection into the active region.

3. CONCLUSIONS

In conclusion our primary objective of demonstrating single, electrically injected InGaN/GaN nanowires was not achieved. Over the course of this project, we gained a number of insights into the primary challenges and roadblocks to achieving this goal. Below some of the primary insights are detailed:

- For radial NW laser, optimization of growth and the heterostructure is difficult due to 3D structure and small size. Basic details such as layer thickness require complex scanning TEM experiments, and doping levels cannot be determined from Hall measurements. Good doping (particularly the p-doped layer) and high quantum efficiency from the MQWs are needed, along with the proper dimensions for the core and shell layers to maximize the confinement factor. However, these characteristics are not easily obtained in the nanowire geometry which stymies optimization.
- Non-uniform growth on nanowire sidewalls from top-to-bottom, both in growth rate and indium incorporation, results in reduced gain and additional losses
- Contact formation leads to significant optical losses. However, a fraction of the wires maintained optically pumped lasing after contact formation. Further study and new schemes and potentially different metals need to be considered to minimize optical losses while simultaneously maximizing carrier injection.
- Nanoscale 3D Ohmic contacts are significantly more challenging to realize than bulk 2D contacts, particularly the p-type contact. Further work is needed to solve this challenge.

Although electrically injected lasing was not demonstrated, this program resulted in a number of technical accomplishments and successes, many of which are detailed in this report and resulting journal publications. Some highlights include:

- Advanced the state-of-the art in controlled III-nitride nanowire fabrication using e-beam patterning and optimized dry and wet etch processes
- Demonstrated processes for nanowire cross-sectional shape control and resulting ability to manipulate nanowire laser properties, such as beam shape and polarization
- Analyzed and gained an understanding of the pros and cons of axial versus radial nanowire laser designs
- Achieved optically pumping lasing from nonpolar core-shell III-N nanowires, demonstrating its viability for electrically injected lasing
- Achieved electrically injected axial and radial InGaN/GaN nanowire LEDs
- Studied impact of metal contacts on optical loss

Additionally, this program contributed to the publication of ten journal articles (eight published, two in preparation), 28 invited talks, and 4 patent applications (see Appendices). Further technical accomplishments and details can be found in the referenced journal articles in Appendix A.

4. REFERENCES

1. X. F. Duan, Y. Huang, R. Agarwal, C. M. Lieber, "Single-nanowire electrically driven lasers"*, Nature*, ***421***, 241 **(2003)**.
2. Q. Li, K. R. Westlake, M. H. Crawford, S. R. Lee, D. D. Koleske, J. J. Figiel, K. C. Cross, S. Fathololoumi, Z. Mi, G. T. Wang, "Optical performance of top-down fabricated InGaN/GaN nanorod light emitting diode arrays"*, Opt. Express*, ***19***, 25528 **(2011)**.
3. J. J. Wierer, Q. Li, D. D. Koleske, S. R. Lee, G. T. Wang, "III-nitride core–shell nanowire arrayed solar cells"*, Nanotechnology*, ***23***, 194007 **(2012)**.
4. D. Li, C. Z. Ning, "Electrical Injection in Longitudinal and Coaxial Heterostructure Nanowires: A Comparative Study through a Three-Dimensional Simulation"*, Nano Lett.*, ***8***, 4234 **(2008)**.
5. H. M. Ng, D. Doppalapudi, E. Iliopoulos, T. D. Moustakas, "Distributed Bragg reflectors based on AlN/GaN multilayers"*, Appl. Phys. Lett.*, ***74***, 1036 **(1999)**.
6. H. Xu, A. Hurtado, J. B. Wright, C. Li, S. Liu, J. J. Figiel, T.-S. Luk, S. R. J. Brueck, I. Brener, G. Balakrishnan, Q. Li, G. T. Wang, "Polarization control in GaN nanowire lasers"*, Optics Express*, ***22***, **(2014)**.
7. Q. Li, J. B. Wright, W. W. Chow, T. S. Luk, I. Brener, L. F. Lester, G. T. Wang, "Single-mode GaN nanowire lasers"*, Optics Express*, ***20***, 17873 **(2012)**.
8. J. B. Wright, S. Campione, S. Liu, J. A. Martinez, H. Xu, T. S. Luk, Q. Li, G. T. Wang, B. S. Swartzentruber, L. F. Lester, I. Brener, "Distributed feedback gallium nitride nanowire lasers"*, Appl. Phys. Lett.*, ***104***, 041107 **(2014)**.

APPENDIX A: PUBLICATIONS RESULTING FROM THIS WORK

1. C. Li et al., "Nonpolar InGaN/GaN multi-quantum-well core-shell nanowire lasers," *in preparation*
2. C. Li et al., "Linearly Polarized Emission from Single Rectangular Cross-sectional Gallium Nitride Nanowire Lasers," *in preparation*
3. C. Li, S. Liu, A. Hurtado, J. B. Wright, H. Xu, T. S. Luk, J. J. Figiel, I. Brener, S. R. Brueck, G. T. Wang, "Annular-Shaped Emission from Gallium Nitride Nanotube Lasers"*, ACS Photonics*, (2015).
4. S. Liu, C. Li, J. J. Figiel, S. R. Brueck, I. Brener, G. T. Wang, "Continuous and dynamic spectral tuning of single nanowire lasers with subnanometer resolution using hydrostatic pressure"*, Nanoscale*, *7*, 9581 (2015).
5. J.B. Wright et al., "Gallium Nitride Distributed Feedback Nanowire Lasers*" Appl. Phys. Lett.* **104**, 041107 (2014); doi: 10.1063/1.4862193
6. C. Guclu, T. S. Luk, G. T. Wang, F. Capolino, "Radiative emission enhancement using nano-antennas made of hyperbolic metamaterial resonators"*, Appl. Phys. Lett.*, ***105***, 123101 (2014). (COVER ARTICLE)
7. H. Xu, A. Hurtado, J. B. Wright, C. Li, S. Liu, J. J. Figiel, T.-S. Luk, S. R. J. Brueck, I. Brener, G. Balakrishnan, Q. Li, G. T. Wang, "Polarization control in GaN nanowire lasers", *Optics Express*, 22, (2014)
8. Weng W. Chow, Frank Jahnke and Christopher Gies, *"*Emission properties of nanolasers during transition to lasing," *Light: Science & Applications,* 3 (2014): e201 (2014)
9. Hurtado et al., "Transverse Mode and Polarization Switching in GaN Nanowire Lasers" *Appl. Phys. Lett.* **103**, 251107 (2013); doi: 10.1063/1.4835115
10. Wright et al. "Multi-Colour Nanowire Photonic Crystal Laser Pixels" *Scientific Reports* 3 : 2982 | DOI: 10.1038/srep02982 (2013)

APPENDIX B: INVITED PRESENTATIONS

1. G.T. Wang, *III-Nitride Nanowires for Solid-State Lighting,* McGill Workshop Emerging Lighting Solutions, Montreal, Canada, 1/10/2013 (keynote)
2. G.T. Wang, *Nanowires: A New Architecture for Solid-State Lighting*, USC Invited Seminar, USC, Los Angeles, CA, 3/6/2013 (invited)
3. G.T Wang, *Nanowires as an Architecture for Solid-State Lighting*, Taiwan SSL Conference, Taipei, Taiwan, 3/26-27/2013 (invited)
4. Wang, G. T., *Nanowires for Solid-State Lighting,* EFRC PI Meeting, 7/18/13, Washington, DC**.**
5. G.T. Wang, *Nanowires: A Future Architecture for Solid-State Lighting,* Fall 2013 National ACS Meeting, 9/8-12/13, Indianapolis, IN.
6. Wright, J. B.,…, G. T. Wang, *Characterization of III-Nitride Nanowires,*Triennal CINT Review, 9/10-11/13, Los Alamos, NM **(invited)**.
7. G.T. Wang, *III-Nitride Nanowires: New Materials for Light Emission*, Nanowires 2013, 11/11-15/13, Rehovot, Israel
8. G. T. Wang, *III-nitride nanowires for visible optoelectronics*, 8th Workshop on Frontiers in Electronics, 12/17-20/13, San Juan, Puerto Rico.
9. Chow, W. W., *Emission properties from nanolasers during transition to lasing,* 44rd Winter Colloquium on the Physics of Quantum Electronics, 1/6-9/14, Snowbird, UT**.**
10. G. T. Wang, *III-nitride nanowires for future optoelectronics*, Arizona State University, 3/27/14, Tempe, AZ
11. I. Brener, *Waves, Light and Artificial Lighting*, Science Bowl 2014, 4/25/14, Washington D.C.
12. Chow, W. W., *Emission properties from nanolasers during transition to lasing,* University of Texas Arlington, EECE Department Seminar, March 21, 2014, Arlington, TX**.**
13. Chow, W. W., *Emission properties from nanolasers during transition to lasing,* SPIE Photonics Europe Conference, 4/14-17/14, Brussels, Belgium**.**
14. Chow, W. W., *Nanolaser*, Workshop in Honor of Dr. Stephen F. Jacobs (co-inventor, Cesium laser, 1962), 1/14-15/2014, Texas A&M University, College Station, TX
15. Wang, G. T., *III-Nitride Nanowire Heterostructures by Top-Down and Combined Top-Down Bottom-Up Approaches,* North American Molecular Beam Epitaxy Conference (NAMBE 2013), 10/5-11/13, Banff, Canada
16. Wang, G. T., *III-Nitride Nanowires: Novel Materials for Light Emission,* AVS 60th International Symposium and Exhibition, 10/27-11/1/13, Long Beach, CA
17. Wang, G. T., *III-Nitride Nanowires: New Materials for Light Emission,* Nanowires 2013, 11/11-15/13, Rehovot, Israel
18. Wang, G. T., *III-Nitride Nanowires for Visible Optoelectronics,* 8th Workshop on Frontiers in Electronics (WOFE 2013), 12/17-20/13, San Juan, Puerto Rico
19. Wang, G. T., *III-Nitride Nanowires for Future Optoelectronics,* Seminar at Arizona State University, 3/27/14, Tempe, AZ
20. Wang, G. T., et al., *Top-Down III-Nitride Nanowires: from LEDs to Lasers,* SPIE Optics+Photonics Meeting, 8/18-21/14, San Diego, CA

21. Fischer, A. J., et al., *Fabrication of InGaN Quantum Dots for Use as Active Photonic Emitters,* SPIE Optics+Photonics 2014 Conference, 8/17-21/14, San Diego, CA
22. Wang, G. T., J. B. Wright, H. Xu, A. Hurtado, C. Li, S. R. J. Brueck, Q. Li, T.-S. Luk, J. J. Figiel, I. Brener, *Mode and Polarization Control in Gallium Nitride Nanowire Lasers,* 2014 Progress in Electromagnetics Research Symposium (PIERS 2014), 8/25-28/2014, Guangzhou, China
23. Wang, G. T., *III-Nitride Nanowires for Future Optoelectronics,* International Symposium on Materials for Enabling Nanodevices (ISMEN2014), 9/3-5/14, Tainan, Taiwan
24. Wang, G.T., *III-Nitride Nanowires: Novel Materials for Future Optoelectronics*, International Symposium on Semiconductor Light Emitting Devices (ISSLED 2014), 12/14-19/15, Kaohsiung, Taiwan
25. Wang, G. T. , *III-Nitride Nanowires for UV-Visible Optoelectronics,* 2015 IEEE Photonics Society Summer Topicals Meeting Series, 7/13-15/15, Nassau, Bahamas
26. Chow, W. W., F. Jahnke, C. Gies, *Nanolaser Emission under Few-Emitter or Unity-Spontaneous-Emission-Factor Conditions,* 12th Conference on Nonlinear Optics and Excitation Kinetics in Semiconductors (NOEKS), 9/22-25/14, Bremen, Germany
27. Chow, W. W., F. Jahnke, C. Gies, *First Principle Study of Nanolasers: Photon Statistics and Laser Threshold,* Asia Communications and Photonics Conference (ACP 2014), 11/11-14/14, Shanghai, China
28. Chow, W. W., *Correlations and Photon Statistics in Nanocavity Emitters,* Nanoscience Seminar Series, Department of Physics, ASU, 4/24/15, Tempe, AZ

DISTRIBUTION

1	MS0957	Jeremy B. Wright (electronic copy)	5331
1	MS1082	Sheng Liu (electronic copy)	1765
1	MS1082	Igal Brener (electronic copy)	1765
1	MS1086	George T. Wang (electronic copy)	1126
1	MS1086	Benjamin Leung (electronic copy)	1126
1	MS1086	Jeffrey J. Figiel (electronic copy)	1126
1	MS1086	Daniel D. Koleske (electronic copy)	1126
1	MS1086	Robert M. Biefeld (electronic copy)	1126
1	MS1086	Richard P. Schneider (electronic copy)	1120
1	MS1086	Mary H. Crawford (electronic copy)	1100
1	MS1086	Weng W. Chow (electronic copy)	1117
1	MS1304	Ting-Shan Luk (electronic copy)	1131
1	MS1314	Tzu-Ming Lu (electronic copy)	1117
1	MS1421	Jeffrey Y. Tsao (electronic copy)	1120

1	MS0359	D. Chavez, LDRD Office	1911
1	MS0899	Technical Library	9536 (electronic copy)


Sandia National Laboratories